Stereoelectronic effects in force-accelerated retro-Diels–Alder reactions

DOI:
10.1055/a-1799-7517

Document Version
Accepted author manuscript

Published in:
SYNLETT

Stereoelectronic effects in force-accelerated retro-Diels–Alder reactions

Lik Chun Wu [a]
Guillaume De Bo*[a]

[a] Department of Chemistry, University of Manchester, Oxford Road, Manchester, M13 9PL, United Kingdom

* guillaume.debo@manchester.ac.uk

Click here to insert a dedication.

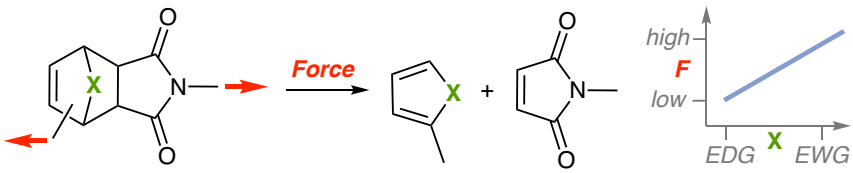

Received:
Accepted:
Published online:
DOI:

Abstract In polymer mechanochemistry, mechanosensitive molecules (mechanophores) are activated upon elongation of anchored polymer arms. The reactivity of a mechanophore can be influenced by a variety of structural factors, including the geometry of attachment of the polymer arms and the nature of eventual substituents. Here we investigate stereoelectronic effects in force-accelerated Diels–Alder reactions using the CoGEF (Constrained Geometries simulate External Force) calculation method. We found that the presence of an electron-donating heteroatom on the diene leads to a lower activation force, and that the mechanochemical reactivity is suppressed when the anchor group is attached to a central rather than lateral position.

Key words Polymer mechanochemistry, mechanophore, force, Diels–Alder, retrocycloaddition, Hammett parameter

In polymer mechanochemistry, polymer arms are used to pull on a central reactive unit (a mechanophore) in order to trigger a chemical transformation.[1] This mechanochemical process is affected by the ease at which the force couples to the reactive bond(s) and, depending on how efficient this mechanochemical coupling is, can lead to an enhancement or reduction in reactivity.[2] Several factors have been shown to affect reactivity under tension such as: the polymer architecture,[3] the nature of the linker[4] and substituents,[5] the stereo-,[2,5d,6] regio-,[2,7] and topochemistry,[8] or even the isotope composition.[9] We[2] and Craig[6a] have previously investigated the influence of regio- and stereochemistry on the dissociation of furan/maleimide Diels–Alder adducts (Figure 1). Here we used CoGEF (Constrained Geometries simulate External Force)[11] calculations to investigate how stereoelectronic effects influence the force-accelerated retro-Diels–Alder (rDA) of related adducts, which differ by the nature of the bridging heteroatom X in the diene, and by the position of the anchor points (Figure1). We found that the dissociation force correlates with Hammett's resonance parameter (σ_{para}) of X, as electron-donating substituents lead to lower activation force. We also found that the mechanochemical reactivity is suppressed when the anchor group is attached to a central rather than lateral position.

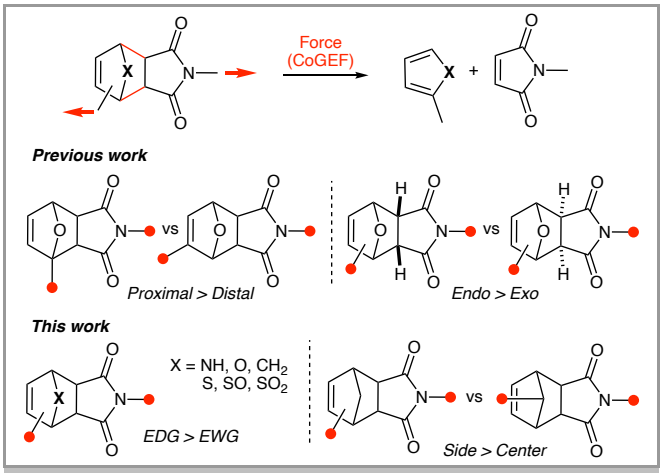

Figure 1. Geometry and stereoelectronic effects in force-accelerated retro-Diels–Alder reactions. Scissile bonds shown in red. Red dots indicate the anchor atoms.

We started our investigation by exploring the effect of substituent X on the mechanical reactivity of four geometrical isomers of a maleimide-based Diels–Alder adduct (Figure 1 and 3a). They differ by the position of the anchor methyl group of the diene (*proximal* or *distal* to the nearest scissile bond) and the stereochemistry of the adduct (*endo* or *exo*). We have previously shown that the *proximal* isomers of the furan/maleimide adduct (X=O) were more reactive than their *distal* counterparts to the extent that the *distal-exo* isomer is mechanically inert.[2] This latter result was confirmed with all the other substituents X explored here (see SI), so our discussion will focus on the other three isomers.

We used CoGEF (Constrained Geometries simulate External Force) calculations (DFT B3LYP/6-31G*) to simulate the mechanical activation of these adducts.[11] This technique works

by incrementally increasing the distance separating two anchor atoms (D, Figure 2) in the mechanophore and minimizing the energy after every iteration. As well as predicting the position of the scissile bond(s), the resulting elongation-energy curve allows for the determination of the energy (E_{max}) and the force (F_{max}) required to reach the maximal state of deformation before the eventual rupture of a covalent bond (Figure 2). Despite its powerful predictive ability, it must be noted that the CoGEF method doesn't account for dynamic or thermal effects and the predicted reactivity can sometimes diverge from the observed reactivity.[11d]

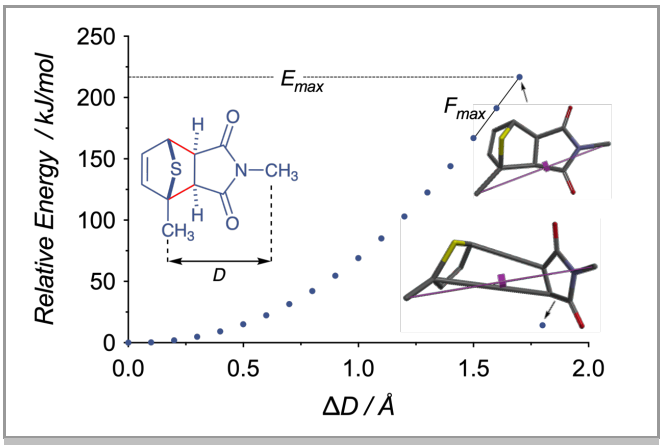

Figure 2. CoGEF calculation (DFT B3LYP/6-31G*) for the S-*prox-exo* adduct. Scissile bonds shown in red. F_{max} is calculated from the slope around E_{max}. Structures at E_{max} and after scission shown (hydrogen atoms omitted for clarity).

The calculated F_{max} were plotted against the Hammett σ_{para} parameter of related functional groups (NHMe, OMe, CHMe, SMe, SOMe, and SO_2Me for X = NH, O, CH_2, S, SO, and SO_2 respectively).[12] We found that the electronic property of X has a substantial influence on the reactivity of the three mechanically active isomers (Figure 3). As the σ_{para} is particularly suited to account for resonance effects, this suggest that the rupture of the scissile bond is facilitated by the presence of a lone pair on X (Figure 4a). Indeed, we found that the pyrrole-maleimide adduct dissociates at the lowest F_{max} when the lone pair is anti-periplanar to the scissile bond (Figure 4a). The presence of a methyl group on the nitrogen places the lone pair in a periplanar position, which prevent the interaction with the σ* of the scissile bond. As a result, F_{max} increases to the level of the carbon derivatives (Figure 4b).

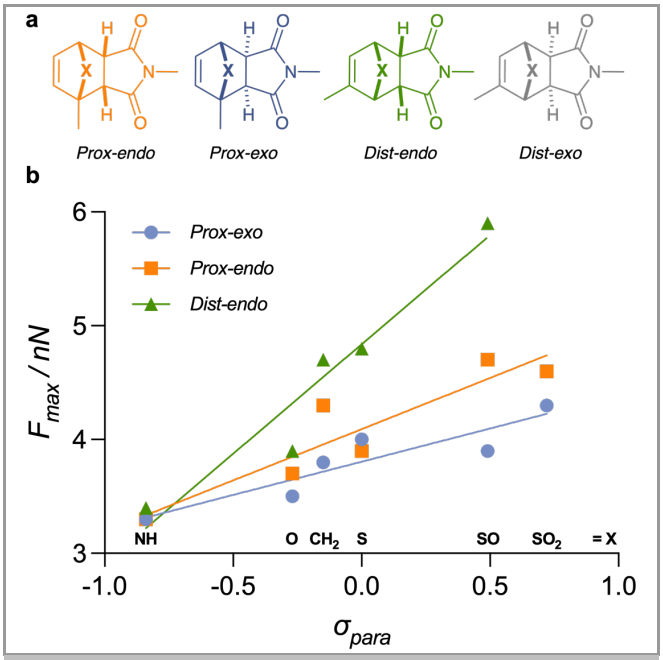

Figure 3. Force dependence on the electronic properties (σ_{para}) of the X substituent. Solid lines correspond to a linear fit (slope/R^2 = 0.584/0.823, 0.900/0.849, and 1.92/0.933 for *Prox-exo*, *Prox-endo*, and *Dist-endo* respectively.

The electronic effect is more pronounced in the least reactive *Dist-endo* isomer than in the most reactive *Prox-exo*. This could be due to the lower mechanochemical coupling observed in *Dist-endo* (see SI). The mechanochemical coupling expresses how much the scissile bond is elongated as the mechanophore is stretched. In other words, the *Dist-endo* requires a higher deformation of the mechanophore to achieve the same elongation of the scissile bond. Hence, one might expect the activation effect of the electron-donating substituent to have a greater influence of the mechanical reactivity of this adduct than the more reactive *proximal* isomers.

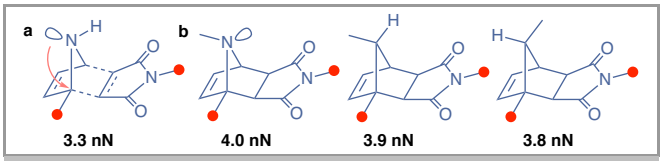

Figure 4. Effect of lone pair orientation on the activation. Red dots indicate the anchor atoms.

On the other side of the scale, the electron-withdrawing substituents (X = SO, SO_2) lead to some unexpected behaviours. The SO_2-*Dist-endo* adduct doesn't undergo a rDA reaction but rather SO_2 is extruded upon planarization of the adduct (see SI).[13] Unlike most of the other adducts where both scissile bonds cleave at once (Figure 1a), the simulated elongations of the SO- and SO_2-*Prox-exo* suggest a stepwise process where the scissile bond nearest to the anchor cleaves first.

These results shed some light on the nature of the force-accelerated retro-Diels–Alder reaction. Many mechanophores described to date are designed around an (apparent) pericyclic mechanism.[14] However, force-promoted retrocycloadditions can proceed via a concerted (like its thermal counterpart) or a stepwise mechanism with various levels of asynchronicity in

between.[11d] Although one must be cautious about inferring mechanistic information from CoGEF profiles, it looks plausible for the rDA to proceed with an increasing level of asynchronicity with a ionic or radical character as the value σ_{para} diverge from 0 toward negative or positive values respectively.[15]

Finally, we explored alternative pulling geometries with NMe and CHMe *exo* and *endo* adducts (Figure 5), but none of these adducts is predicted to undergo a rDA reaction due to a poor mechanochemical coupling of these bonds. It originates from a poor alignment of the putative scissile bonds (*a* and *b*, Figure 5) with the force vector (see SI). The coupling is further diminished by the symmetrical arrangement of the anchor, which spreads the strain equally over the molecular backbone.[8a]

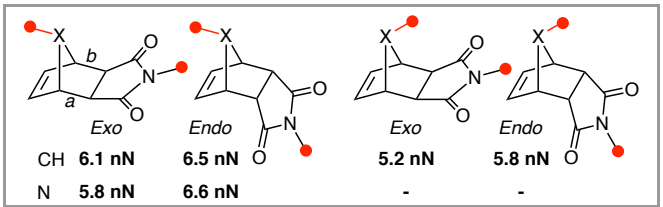

Figure 5. Alternative pulling geometries. Scissile bond shown in red. Red dots indicate the anchor atoms.

In conclusion, we have investigated the mechanical reactivity of several diene-maleimide Diels–Alder adducts varying by the nature of the bridging heteroatom and the position of the pulling anchors. We have found that the activation force correlates with Hammett's resonance parameter (σ_{para}). The lowest activation force was observed for the most electron donating substituent (NH) due to labialization of the scissile bond by the heteroatom's lone pair. We have also found that symmetrically placed anchors were detrimental for the mechanical activation because the resulting strain is spread equally over the molecular skeleton, effectively reducing the mechanochemical coupling with the putative scissile bond. These stereoelectronic effects complete our previous investigation of the factors affecting the reactivity of these DA mechanophores where the effect of geometry was explored.[2] The general principles uncovered in these studies should be applicable to reactivity of other mechanophores.

Funding Information

G.D.B. is a Royal Society University Research Fellow.

Supporting Information

YES

Primary Data

NO.

Conflict of Interest

The authors declare no conflict of interest.

References and Notes

(1) (a) O'Neill, R. T.; Boulatov, R. *Nat. Rev. Chem.* **2021**, *5* (3), 148–167. (b) De Bo, G. *Macromolecules* **2020**, *53* (18), 7615–7617. (c) Caruso, M. M.; Davis, D. A.; Shen, Q.; Odom, S. A.; Sottos, N. R.; White, S. R.; Moore, J. S. *Chem. Rev.* **2009**, *109*, 5755–5798.

(2) Stevenson, R.; De Bo, G. *J. Am. Chem. Soc.* **2017**, 139, 16768-16771.

(3) (a) Noh, J.; Peterson, G. I.; Choi, T. *Angew. Chem. Int. Ed.* **2021**, *60*, 18651–18659. (b) Peterson, G. I.; Lee, J.; Choi, T.-L. *Macromolecules* **2019**, *52*, 9561–9568. (b) Lin, Y.; Zhang, Y.; Wang, Z.; Craig, S. L. *J. Am. Chem. Soc.* **2019**, *141*, 10943–10947. (c) Church, D. C.; Peterson, G. I.; Boydston, A. J. *ACS Macro Lett.* **2014**, *3*, 648–651. (d) Zhang, H.; Diesendruck, C. *Angew. Chem. Int. Ed.* **2022**. DOI: 10.1002/anie.202115325.

(4) (a) Stevenson, R.; Zhang, M.; De Bo, G. *Polym. Chem.* **2020**, *11* (16), 2864–2868. (b) Wang, J.; Kouznetsova, T. B.; Kean, Z. S.; Fan, L.; Mar, B. D.; Martinez, T. J.; Craig, S. L. A *J. Am. Chem. Soc.* **2014**, *136*, 15162–15165. (c) Klukovich, H. M.; Kouznetsova, T. B.; Kean, Z. S.; Lenhardt, J. M.; Craig, S. L. A *Nat. Chem.* **2013**, *5*, 110–114. (d) Tian, Y.; Boulatov, R. *ChemPhysChem* **2012**, *13*, 2277–2281. (e) Klukovich, H. M.; Kean, Z. S.; Ramirez, A. L. B.; Lenhardt, J. M.; Lin, J.; Hu, X.; Craig, S. L. *J. Am. Chem. Soc.* **2012**, *134*, 9577–9580.

(5) (a) Brown, C. L.; Bowser, B. H.; Meisner, J.; Kouznetsova, T. B.; Seritan, S.; Martinez, T. J.; Craig, S. L. *J. Am. Chem. Soc.* **2021**, *143*, 3846. (b) Nixon, R.; De Bo, G. *Nat. Chem.* **2020**, *12*, 826–831. (c) Lin, Y.; Craig, S. L. *Chem. Sci.* **2020**, *11*, 10444–10448. (d) Barbee, M. H.; Kouznetsova, T.; Barrett, S. L.; Gossweiler, G. R.; Lin, Y.; Rastogi, S. K.; Brittain, W. J.; Craig, S. L. *J. Am. Chem. Soc.* **2018**, *140*, 12746–12750. (e) Kryger, M. J.; Munaretto, A. M.; Moore, J. S. *J. Am. Chem. Soc.* **2011**, *133*, 18992–18998.

(6) (a) Wang, Z.; Craig, S. L. *Chem. Commun.* **2019**, *50*, 2836. (b) Zhang, H.; Li, X.; Lin, Y.; Gao, F.; Tang, Z.; Su, P.; Zhang, W.; Xu, Y.; Weng, W.; Boulatov, R. *Nat. Commun.* **2017**, *8*, 1147. (c) Wang, J.; Kouznetsova, T. B.; Craig, S. L. *J. Am. Chem. Soc.* **2015**, *137*, 11554–11557. (d) Kean, Z. S.; Niu, Z.; Hewage, G. B.; Rheingold, A. L.; Craig, S. L. *J. Am. Chem. Soc.* **2013**, *135*, 13598–13604. (e) Lenhardt, J. M.; Ong, M. T.; Choe, R.; Evenhuis, C. R.; Martinez, T. J.; Craig, S. L. *Science* **2010**, *329*, 1057–1060.

(7) (a) Lin, Y.; Barbee, M. H.; Chang, C.-C.; Craig, S. L. *J. Am. Chem. Soc.* **2018**, *140*, 15969–15975. (b) Kim, T. A.; Robb, M. J.; Moore, J. S.; White, S. R.; Sottos, N. R. *Macromolecules* **2018**, *51*, 9177–9183. (c) Robb, M. J.; Kim, T. A.; Halmes, A. J.; White, S. R.; Sottos, N. R.; Moore, J. S. *J. Am. Chem. Soc.* **2016**, *138*, 12328–12331. (d) Gossweiler, G. R.; Kouznetsova, T. B.; Craig, S. L. *J. Am. Chem. Soc.* **2015**, *137*, 6148–6151. (e) Konda, S. S. M.; Brantley, J. N.; Varghese, B. T.; Wiggins, K. M.; Bielawski, C. W.; Makarov, D. E. *J. Am. Chem. Soc.* **2013**, *135*, 12722–12729.

(8) (a) Zhang, M.; De Bo, G. *J. Am. Chem. Soc.* **2020**, *142*, 5029–5033. (b) Zhang, M.; De Bo, G. *J. Am. Chem. Soc.* **2019**, *141*, 15879–15883. (c) Zhang, M.; De Bo, G. *J. Am. Chem. Soc.* **2018**, *140*, 12724–12727.

(9) Nixon, R.; De Bo, G. *J. Am. Chem. Soc.* **2021**, *143*, 3033–3036.

(10) Wang, J.; Kouznetsova, T. B.; Niu, Z.; Rheingold, A. L.; Craig, S. L. *J. Org. Chem.* **2015**, *80*, 11895.

(11) Beyer, M. *J. Chem. Phys.* **2000**, *112*, 7307–7312. For recent reviews see: (b) Ribas-Arino, J.; Marx, D. *Chem. Rev.* **2012**, *112*, 5412–5487. (c) Stauch, T.; Dreuw, A. *Chem. Rev.* **2016**, *116*, 14137–14180. (d) Klein, I. M.; Husic, C. C.; Kovács, D. P.; Choquette, N. J.; Robb, M. J. J. Am. Chem. Soc. **2020**, *142*, 16364.

(12) McDaniel, D. H.; Brown, H. C. *J. Org. Chem.* **1958**, *23*, 420.

(13) The release of singlet oxygen (see (a) Turksoy, A.; Yildiz, D.; Aydonat, S.; Beduk, T.; Canyurt, M.; Baytekin, B.; Akkaya, E. U. *RSC Adv.* **2020**, *10*, 9182) has been achieved recently using a similar flex-activation mechanism (see (b) Larsen, M. B.; Boydston, A. J. *J. Am. Chem. Soc.* **2013**, *135*, 8189.)

(14) Izak-Nau, E.; Campagna, D.; Baumann, C.; Göstl, R. Polym. Chem. **2020**, *11*, 2274.

(15) For a computational mechanistic study of force-accelerated rDA, discussing the synchronicity of the process see: Cardosa-Gutierrez, M.; De Bo, G.; Duwez, A.-S.; Remacle, F. *ChemRxiv* **2022**. DOI: 10.26434/chemrxiv-2022-g64jp.